CREEP RUPTURE ANALYSIS OF A BEAM RESTING ON HIGH TEMPERATURE FOUNDATION

Randy J. Gu*
Oakland University
Rochester, Michigan 48063

Francis A. Cozzarelli
State University of New York at Buffalo
Buffalo, New York 14260

In this research, a simplified uniaxial strain-controlled creep damage law is deduced with the use of experimental observation from a more complex strain-dependent law. This creep damage law correlates the creep damage, which is interpreted as the density variation in the material, directly with the accumulated creep strain. Based on the deduced uniaxial strain-controlled creep damage law, a continuum mechanical creep rupture analysis is carried out for a beam resting on a high temperature elastic (Winkler) foundation. The analysis includes the determination of the nondimensional time for initial rupture, the propagation of the rupture front with the associated thinning of the beam, and the influence of creep damage on the deflection of the beam. Creep damage starts accumulating in the beam as soon as the load is applied, and a creep rupture front develops at and propagates from the point at which the creep damage first reaches its critical value. By introducing a series of fundamental assumptions within the framework of technical Euler-Bernoulli type beam theory, a governing set of integro-differential equations is derived in terms of the nondimensional bending moment and the deflection. These governing equations are subjected to a set of interface conditions at the propagating rupture front. A numerical technique is developed to solve the governing equations together with the interface equations, and the computed results are presented and discussed in detail.

1. INTRODUCTION

Tertiary creep involves the process of fracture leading ultimately to complete failure, and is associated with local reduction in cross-sectional area and more importantly with the nucleation and growth of voids and microracks along grain boundaries. This failure mode leads to eventual collapse of a structural component and is known in the literature as creep rupture or stress rupture. In order to meet the demands of designers and engineers concerned with the safety of equipment operating at elevated temperatures, researchers in recent decades have conducted extensive creep rupture experiments from which they hope to extract some useful "extrapolation" parameters. Such parameters are inevitably limited by the laboratory-allowed time scale and by the usual scatter of the empirical data, but they are employed to estimate the appropriate stress and temperature requirements for the practical service lives of equipment in operation. Amongst such extrapolation parameters methods are the ones of Larson-Miller (1952) [1], Manson-Haferd (1953) [2], Orr-Sherby-Dorn (1954) [3], and many others. Manson and Ensign [4] have presented an interesting review on the progress in extrapolation procedures for creep rupture; an excellent discussion of these is also given in the text by Conway [5].

In parallel with the development cited above, other researchers including some metallurgists have attempted to define and quantify a suitable variable which describes the damage state and measures the extent of damage in materials undergoing creep. The major hurdle in this line of research is the manner by which ones bridges the gap between the scalar damage variable obtained by macroscopic creep testing and the microscopic processes involved in the nucleation and growth of voids and microcracks at grain boundaries. Such variables are expected to be able to characterize the damage state from

the physical and quantitative points of view, and furthermore to provide a useful tool for analytical modelling via continuum mechanics. Amongst such approaches are Robinson's linear cumulative creep damage law (1952) [6], Hoff's ductile creep rupture theory (1953) [7], Kachanov's brittle rupture theory (1961) [8], Robotnov's coupled damage creep theory (1969) [9], and many other modified theories such as the one due to Leckie and Hayhurst (1974) [10]. Comparative studies of the various theories may be found in [11-13]. Recently, scientists have observed a close relation between density change and the nucleation and growth of voids and microcracks associated with creep damage in polycrystalline materials. Extensive efforts have thus been made to identify and quantify creep damage in terms of the density variation which is attributed to cavitation in a creeping material. Following this concept, Piatti et al [14] developed a refined experimental technique to measure the density variation for use as a definition of creep damage. Using data obtained in this manner for steel, Belloni et al [15,16] proposed a statistically-based damage law in a complicated power law form similar to the one presented in Woodford's parametric study of creep damage [17].

Because of its inherent mathematical complexity, the creep damage law proposed in [15,16] is somewhat inconvenient for analytical treatment within the framework of continum creep damage mechanics. In addition, some arbitrariness remains in the determination of the material constants appearing in this damage law (see [18]). Accordingly, the first task in this work is to obtain a simplified yet still useful damage law. This task is addressed in Section 2 where we argue first from the microscopic point of view that density variation certainly is a proper index of damage in a material undergoing creep deformation. We then propose a simplified uniaxial strain-controlled damage law by introducing some assumptions based on experimental observation

associated with the original damage law, and this strain-controlled damagelaw is demonstrated to be closely related not only to the original damage law but also to Kachanov's damage law (see [8]). We conclude Section 2 with the observation that, whereas a typical boundary value problem suffices to represent the problem in "the first stage of creep damage", we encounter in "the second stage of propagation of the rupture front" a moving boundary problem similar to the Stefan problem in heat conduction [19].

Utilizing the above strain-controlled creep damage theory, we present in Section 3 a continuum mechanics model for the creep rupture analysis of a beam resting on a high temperature elastic Winkler foundation which generates a prescribed thermal gradient in the thickness direction. Based on technical Euler-Bernoulli-type beam theory, we derive in Section 3 a set of governing differential equations for a region with a moving boundary (rupture front) which is prescribed by a set of interface equations. Owing to the inherent nonlinearity of the problem, closed form solutions generally do not exist. Accordingly, a successful treatment of the problem requires the application of a suitable numerical technique which is then presented in Section 4. In the latter part of Section 4, we consider a simple case for which a closed form solution does exist. We then present detailed numerical results for the problems in which temperature gradient is taken into account and the foundation is either present or absent. The results consist of the nondimensional forms for bending moment, deflection, and the geometric shapes of the rupture front.

2. STRAIN-CONTROLLED CREEP DAMAGE

2.1 Creep Damage Law Under Uniaxial Stress

Virtually all load-bearing structural components operating at elevated

temperatures undergo the typical 3-stage creep phenomenon. Various phenomenological interpretations of the creep process have been devised, usually employing the concept that creep is essentially a competition between strain-hardening and recovery [20]. It is well understood that at elevated temperatures a crystalline solid may deform in accordance with several mechanisms such as dislocation creep and diffusion creep. Each such mechanism is most active is some range of stress and temperature [21], such that within certain regions of the stress-temperature space one mechanism is said to dominate the others. The pictorial maps constructed by this concept are known as Ashby's deformation-mechanism maps [21,22]. Raj and Ashby [23] have pointed out that the creep mechanisms mentioned above are in fact an "accommodation process" for grain boundary sliding. When a shear stress causes sliding to occur at a generally nonplanar grain boundary, some accommodation process (such as diffusional flow or plastic flow) is necessary to heal the crystalline structure at the deviation of the boundary from a perfect plane. In the event that this accommodation process does not develop fully at a boundary deviation during sliding, an "incompatibility" results in the form of voids and wedge cracks along the grain boundaries which are oriented roughly perpendicular to the tensile axis. As the material is strained further the coalescence of voids and cracks eventually leads to intergranular creep fracture. Clearly, as the cavity volume increases during the process of tertiary creep and eventual fracture, the material dilates. In this section, we shall focus on a strain-controlled constitutive continum damage law based on this close relation between creep damage and cavitation induced dilation in materials.

The type of damage described above is associated with power-law or dislocation creep [23,24]. Steady dislocation creep under constant uniaxial tensile stress σ_o is found experimentally to obey the constitutive

relation[25]

$$\dot{\varepsilon}_s = A(T)\,\sigma_o^n \tag{1}$$

in which n is the constant stress power. The reciprocal viscosity coefficient A(T) is expressed as the Arrhenius equation

$$A(T) = A^* \exp(-\Delta H/RT) \tag{2}$$

where A^* is the relatively temperature insensitive pre-exponential cofficient, ΔH the activation energy for creep, R the gas constant and T the absolute temperature. Equation (1), which is also known as Norton's steady creep law, will be employed to describe the creep deformation process in the problem considered later in this work.

From the phenomenological point of view, creep rupture can be separated into two categories. Failure at high stress and low temperature is characterized by pronounced lateral contractions and the first continuum model for this process is known as Hoff's ductile creep rupture theory [7]. On the other hand, low stress levels together with high temperatures result in brittle type of rupture with little lateral contraction, and the first phenomenological theory for this process was formulated by Kachanov [8]. We shall not consider Hoff's theory further here (ample discussion is given in [13,26]), but we shall now review Kachanov's theory briefly. Kachanov defined the damage variable ω for a one-dimensional test specimen in accordance with

$$\omega = \frac{A_o - A_e}{A_o} = 1 - \frac{A_e}{A_o}$$

where A_o and A_e are, respectively, the original and the effective cross sectional areas carrying the load. Clearly, cavitation creates new internal surface area which in turn reduces the effective cross-sectional area carrying the load. Thus, the material in its virgin state has the damage ω equal to zero, while the damage in a completely deteriorated material approaches unity. A power law for the damage-rate was postulated by Kachanov for variable one-dimensional stress as

$$\dot{\omega} = C\left[\frac{\sigma}{1-\omega}\right]^{\nu} \tag{3}$$

where C, ν are material constants, and where C may be temperature dependent. Assuming that the material is initially undamaged, integration of the above equation gives

$$1 - (1-\omega)^{\nu+1} = C(1+\nu)\int_0^t \sigma^{\nu}(t')dt' \tag{4}$$

As pointed out earlier in this section, a close connection exists between creep damage and the cavitation induced dilation of a material. Belloni et al [15,16] have employed material density variation as the measure of damage in a creep material using refined techniques. They proposed a damage law at constant stress σ_o in the power form for the uniaxial tension test

$$D = c\, \varepsilon_c^{\alpha}\, \sigma_o^{\gamma}\, t^{\delta} \tag{5}$$

where $D = -\Delta\rho/\rho_o$, ρ_o is the density of the material in the virgin state, and $\Delta\rho$ is the change in density due to the volume dilation of the material. In eqn.(5) ϵ_c denotes the creep strain, and c, α,γ,δ appear to be relatively insensitive to temperature, but c is highly temperature sensitive. In analogy with Kachanov's damage variable ω , the damage D has value equal to zero in the virgin state and is equal to a critical value at rupture D_r, which is a material constant. Employing statistical regression techniques, Belloni et al were able to correlate their experimental data with damage law (5). A close inspection in eqn.(5), however, reveals that some arbitrariness exists in the determination of the material constants (for details see [18]). This arbitrariness is a consequence of treating ϵ_c and σ_o as independent state variables in eqn.(5), without considering the constitutive creep law. One possible way of eliminating this arbitrariness is outlined by the sequence of simplifications given below.

First, based on the findings in [16] and related work [26,27] we shall make the simplifyig assumption

$$\gamma = \delta n \tag{6}$$

It will be shown later that eqn.(6) together with $\nu=n$ in eqn.(4) establishes an equivalence between Kachanov's formulation and the current one. We further assume that steady creep as described by eqn.(1) completely dominates the deformation behavior, i.e., the material is non-Newtonean viscous. A combination of eqns.(1) and (5), together with assumption (6), then gives

$$D = \frac{c}{A(T)^{\delta}} (\dot{\epsilon}_s t)^{\alpha+\delta} \tag{7}$$

or

$$D = \frac{C}{A(T)^{\delta}} \varepsilon_s^{\alpha+\delta} \tag{8}$$

in which ε_s is the creep strain under the steady creep condition. It has been found [28] that, for the rupture mechanism considered here, the product of steady-creep-rate, $\dot{\varepsilon}_s$, and the time-to-rupture, t_R, is a constant, i.e.

$$\dot{\varepsilon}_s t_R = C_{MG}$$

where C_{MG} is known as Monkman-Grant constant which has the dimension of strain. This relationship holds true for a wide range of temperature and stress. Therefore, at rupture eqn. (7) gives

$$D_r = \frac{C}{A(T)^{\delta}} (C_{MG})^{\alpha+\delta} \tag{9}$$

where D_r is the critical value of damage at rupture. Belloni et al's data [15] showed that the critical value of damage in the high temperature range is relatively insensitive to temperature. The temperature independent character of both C_{MG} and D_r immplies that the $B/A(T)^{\delta}$ in eqn. (9) must also be temperature independent. Thus

$$\frac{C}{A(T)^{\delta}} = c_o$$

where c_o is a temperature independent material constant. Substituting this back into damage law (8) we then get the simplified form

$$D = c_o \varepsilon_s^{\alpha+\delta} \tag{10}$$

Although a significant simplification has been obtained, damage law (10) is still physically plausible. Note that, although damage is an explicit function of strain along, it is an implicit function of temperature and stress via creep constitutive law (1). In accordance with eqn.(10), a material exposed to stress experiences damage directly related to the creep strain, and rupture occurs as the available creep ductility is exhausted. Hanna and Greenwood [29] showed, for copper with pre-nucleated cavities subjected to low stress and with the creep rate linearly related to the stress, that

$$-\frac{\Delta\rho}{\rho_o} \propto \varepsilon_c \tag{11}$$

Although a surprising analogy appears to exist between eqns. (10) and (11), conclusions may not be easily drawn on the material constants in eqn.(10). However, it does appear very reasonable to postulate that creep damage, as measured by density variation, be expressed explicity as a function of creep strain.

In many engineering practices, however, the stress may be varying with time due to effect such as load variation and stress relaxation. The extension of the original creep damage law, eqn.(5) , to the case of time dependent uniaxial stress has been presented in [30]. In the case of simplified eqn.(10) it suffices to employ the integral form of creep strain for variable stress, and thus integrating $\dot{\varepsilon}_s = A(T)\sigma(t)^n$ we obtain

$$D(t) = C_o \left\{ \int_o^t A(T)\ \sigma^n(t')dt' \right\}^{\alpha+\delta} \tag{12}$$

Here, the reciprocal viscosity function, A(T), is retained inside the integral sign, in order to allow for the situation in which the temperature varies with time. If $\nu=n$ in Kachanov's theory [see eqn.(4)], eqns. (4) and (12) assume a

very similar form; a more detailed comparison of strain-dependent theory with Kachanov's approach is given in [31].

2.2 Propagation of a Creep Rupture Front -- The Moving Boundary Problem

A nonuniform state of stress may be introduced by the irregular geometry of a structure, nonhomogeneous material properties, and nonuniform external loads. Under such circumstances the creep damage within the structure would be a function of the space coordinates in addition to time. Creep damage starts accumulating in the structure as soon as the loads are applied. As time elapses, the creep damage at some point within or on the surface of the structure would first reach the critical value, D_r, at which rupture takes place. This initial rupture time, t_I, is determined in accordance with eqn.(12) as

$$D_r = C_o \left\{ \int_0^{t_I} A(T)\, \sigma^n(t')dt' \right\}^{\alpha+\beta} \qquad (13)$$

A rupture front then develops generally as a smooth surface, and starts propagating through the structure until the entire structure collapses at some time t_{II}. It is readily seen that the lifetime of a structure may be divided into two time intervals or stages, i.e., $0 \leq t < t_I$ and $t_I \leq t < t_{II}$. In the first stage $0 \leq t < t_I$, which has been termed the stage of latent failure by Kachanov [8] or the incubation period by Johnson [32], the creep damage is assumed to be less than the critical value (D_r) everywhere in the structure. In the second stage $t_I \leq t < t_{II}$, which has been termed the stage of propagation of rupture, a rupture front Σ along which

$$D = D_r, \qquad (14)$$

travels through the structure and complete collapse occurs at t_{II}.

A condition on the direction of travel for the rupture front Σ may be obtained by taking the total time derivative of eqn.(14). Accordingly, we obtain

$$\frac{\partial D}{\partial t} + \frac{\partial D}{\partial N}\frac{dN}{dt} = 0$$

in which N designates the coordinate normal to the rupture front. Similarly, the geometry of the rupture front Σ is constrained by

$$\frac{\partial D}{\partial t} + \frac{\partial D}{\partial x_j}\frac{dx_j}{dt} = 0 \qquad (15)$$

in which the x_j are the space coordinates.

This type of problem, more generally called moving (free) boundary problem, is well-known in heat conduction [19] with phase change and is known as the Stefan problem. Although the Stefan problem and the creep rupture problem share analogous mathematical characteristics, there are some significant physical differences. Instead of the temperature profile of the Stefan problem, we are now more concerned about the mechanical behavior of the structure, such as the coupling between the stress redistribution and the speed of the moving boundary (rupture front). Owing to the inherent nonlinearity of the problem, closed form solutions generally do not exist for moving boundary problems with a finite damain. Accordingly, a successful treatment of such problems will require the application of a suitable numerical technique. A thorough discussion and comparison of numerical methods currently used for moving boundary problems is given in [33]. Details of the numerical technique which we shall choose will be disclosed in subsequent sections as the need arises.

3. CREEP RUPTURE IN A BEAM ON A WINKLER FOUNDATION

3.1 Statement of the Problem

The beam problem to be studied is depicted in Fig. 1a. We consider a beam continuously supported by an elastic Winkler foundation, which exerts a restoring force as the beam deflects under the action of a distributed lateral load. Since the foundation is at an elevated temperature, a prescribed thermal gradient is assumed to exist in the z-direction (thickness) of the beam. It is assumed that this prescribed temperature distribution through the thickness of the beam is independent of time during the deformation and rupture processes. The physical model used to analyze the problem is shown in Fig. 1b. Here, the elastic foundation is modelled as an infinite series of infinitesimal springs with an elastic constant K [34], i.e. as an elastic Winkler foundation. Creep deformation starts to accumulate in the beam as soon as the lateral load is applied. In geophysical research this type of flexure model has recently yielded some interesting results on lithospheric flexures (eg. see McMullen et al [35]), where the temperature variation with z is due to the geothermal gradient and the Winkler foundation is due to the underlying mantle. In addition to the creep deformation, we shall also consider the effects of creep damage using the concepts previously developed. In brief, it is our major goal here to explore the propagation of a creep rupture front in a non-isothermal beam under distributed lateral load. During the second stage of damage the beam is thinning in a non-uniform manner, and accordingly the cross-section of the beam is not constant (see Fig. 1c). It will be seen later that a moving boundary problem is encountered as a consequence of this thinning behavior.

The problem presented here is extremely complex in nature. In order to reduce the mathematical difficulties somewhat, we present below a series of

simplifying assumptions. Firstly, we assume that the material in the beam obeys the Norton law of steady creep, with viscosity dependent on the prescribed temperature gradient. Although the beam is of non-uniform cross-section during the second stage of damage, we assume that technical Euler-Bernoulli-type beam theory is valid throughout the entire process of creep damage. We also restrict our consideration to the case of small deformations and small rotations. Furthermore, we assume that no major cracks form in the unruptured segment of the beam during the process of rupture, and thus the effects of stress concentration at crack tips are excluded from the current study. Finally, we assume that the shear stresses are negligibly small when compared with the axial stresses due to flexure.

3.2 Mathematical Formulation of the Problem

The constitutive law governing the creep deformation in the beam is assumed to be of the Norton type [eqn. (1)]:

$$\dot{\varepsilon}_c = A(z)\sigma^n \tag{16}$$

Here the stress state σ may vary with time as well as with the x- and z-coordinates. Note also that the reciprocal viscosity coefficient function $A(z)$ is an implicit function of z via the temperature distribution (see Fig. 1c).

The geometry of the beam is shown is Fig. 1c; it has a rectangular cross-section of width b and thickness h and the length of the beam is 2L. For simplicity we will consider symmetric loading and thus only symmetric deformation in this work, and therefore only half of the span of the beam need be considered. Employing Euler-Bernoulli-type beam theory with h constant, we

may derive the expression for stress in terms of the bending moment M as

$$\sigma = \frac{M}{\mathscr{I}_o}\left(\frac{z-e_o}{A(z)}\right)^{\frac{1}{n}} \tag{17}$$

where e_o is the distance to the neutral axis (marked as N.A. in Fig.1c). Also, the governing equation in the bending moment M is obtained as

$$\frac{\partial^2 M}{\partial x^4 \partial t} + K\left(\frac{M}{\mathscr{I}_o}\right)^n = \frac{\partial^3 P}{\partial x^2 \partial t} \tag{18}$$

where P is the applied lateral load, and we have introduced the notation for flexural rigidity

$$\mathscr{I}_o = b \int_o^{h_o} \left[\frac{z'-e_o}{A(z')}\right]^{\frac{1}{n}} z'dz' \tag{19}$$

The R.H.S. of eqn.(18) vanishes if we assume that the applied lateral load P(x,t) is expressed mathematically in the form

$$P(x,t) = P_o\, f(x)\, H(t) \tag{20}$$

where P_o is the maximum load at x=0, f(x) is the symmetric shape function and H(t) represents the Heaviside unit step function. For a viscous material governed by eqn. (16) we have the initial condition in M as

$$\frac{d^2M(x,0^+)}{dx^2} = -f(x) \tag{21}$$

For further simplicity, we also assume that the beam is simply supported at both ends and that the lateral load vanishes at both ends. Due to the symmetric nature of the problem as previously mentioned, the boundary conditions follow as

$$\frac{\partial M}{\partial x} = \frac{\partial^3 M}{\partial x^3} = 0 \qquad \text{at} \quad x=0 \tag{22a}$$

$$\frac{\partial^2 M}{\partial x^2} = M = 0 \qquad \text{at} \quad x=L \tag{22b}$$

It is important to point out that the neutral axis does not coincide with the centroidal axis in this beam problem since the viscosity is inhomogeneous due to its dependence on a non-uniform temperature distribution [36]. Since the axial force is zero in this problem, the distance to the neutral axis e_o may be determined in the first stage of damage from

$$\int_o^{h_o} \left[\frac{z'-e_o}{A(z')}\right]^{\frac{1}{n}} dz' = 0 \tag{23}$$

It is our task now to extend the above mathematical formulation, which is valid only for the first stage of creep damage, into the second stage of creep damage. The shear stresses in technical beam theory are usually negligibly small when compared with the axial stress. It is thus reasonable to utilize the uniaxial strain-controlled damage law. The creep damage then follows from eqn. (12), which with the use of eqn. (17) yields

$$D(x,z,t) = c_o \left\{\int_o^t \left[\frac{M}{\mathscr{J}_o}\right]^n (z-e_o)\,dt'\right\}^{\alpha+\delta} \tag{24}$$

Experimental evidence [37] has shown that there is virtually no creep damage in a crystalline material under compression. Therefore, the above equation is valid only in the region $e_o<z\leq h_o$ (see Fig. 1c), while the creep damage is assumed to be identically zero in the remainder of the region. The initial rupture time t_I may now be obtained from the implicit relation

$$D_{cr} = c_o \left\{ \int_o^{t_I} \left[\frac{M}{\mathscr{D}_o}\right]^n (z-e_o)dt' \right\}^{\alpha+\delta} \tag{25}$$

where the initial rupture clearly occurs at the midpoint of the bottom fiber (i.e. $x=0$ and $z=h_o$), since it is there that the tensile strain is maximum in magnitude.

Rupture thus starts at the point $x,z=0,h_o$, and then develops into a moving front which in turn causes the beam to thin (see Fig 1c). We shall call the region $0\leq x<\delta(t)$ the thinning zone, and the remaining interval $\delta(t)\leq x\leq L$ the uniform zone since this interval is of uniform thickness. The quantities h and e, which designate the thickness and the distance to the neutral axis within the thinning zone of the beam, are clearly function of x and t. Furthermore, the flexural rigidity $\mathscr{D}$ in the thinning zone is also a function of x and t since it involves h and e. Governing equation (18) with P given by eqn. (20) may now be restated in the thinning zone as

$$\frac{\partial^5 M}{\partial x^4 \partial t} + K\left(\frac{M}{\mathscr{D}}\right)^n = 0 \qquad 0\leq x<\delta(t), \quad t_I\leq t \tag{26a}$$

and in the uniform zone as

$$\frac{\partial^5 M}{\partial x^4 \partial t} + K\left(\frac{M}{\mathscr{D}_o}\right)^n = 0 \qquad \delta(t)<x\leq L, \quad t_I\leq t \tag{26b}$$

where

$$\mathcal{F} = \mathcal{F}(x,t) = b \int_0^{h(x,t)} \left[\frac{z'-e(x,t)}{A(z')}\right]^{\frac{1}{n}} z'dz', \quad 0 \leq x < \delta(t), \quad t_I \leq t \qquad (27)$$

It is readily seen that governing equations (26) are subjected to a moving junction, which separates the thinning zone from the uniform zone. Note that the upper limit h(x,t) and the quantity e(x,t) in integral (27) are changing and unknown functions, and thus we must obtain conditions which govern the variables h,δ, and e. It may be shown that if the rupture front Σ is prescribed as

$$\Sigma : \quad z = h(x,t) \qquad t_I \leq t$$

eqn. (15) can be rewritten as

$$\frac{\partial D}{\partial t} + \frac{\partial h}{\partial t}\frac{\partial D}{\partial z} = 0 \qquad t_I \leq t \qquad (28)$$

Substitution of the expression for damage [eqn. (24)] into the above equation yields after some manipulation

$$\frac{\partial h}{\partial t} = -\left(\frac{M}{\mathcal{F}}\right)^n (h-e) \Big/ \left\{ \int_0^t \left(\frac{M}{\mathcal{F}}\right)^n dt' \right\}, \quad 0 \leq x < \delta(t), \quad t_I \leq t \qquad (29)$$

The creep damage at the junction point Q in Fig. 1c with coordinates $x=\delta(t)$ and $z=h_o$ should be equal to the critical value, i.e.

$$D(x,z,t) = D_{cr}, \qquad x=\delta(t), \qquad z=h_o, \qquad t_I \leq t$$

Following the same procedure employed for eqn. (29), the total time derivative of this equation now gives

$$\frac{d\delta(t)}{dt} = -M^n \Big/ \left\{ n \int_0^t M^{n-1} \frac{\partial M}{\partial x}\, dt' \right\}, \quad x=\delta(t), \quad t_I \le t \tag{30}$$

Note that the quantity $\mathcal{G}(x,t)$ does not appear in the above equation as it is a constant at the junction point Q (see Fig. 1c).

Finally, eqn. (23) for the distance to the neutral axis of the beam now becomes for the second stage of creep damage

$$\int_0^{h(x,t)} \left[\frac{z'-e(x,t)}{A(z')}\right]^{\frac{1}{n}} dz' = 0 , \quad 0 \le x \le \delta(t), \quad t_I \le t$$

Differentiating the above equation with respect to time we obtain the equation

$$\frac{\partial e}{\partial t} = n\left[\frac{h-e}{A(h)}\right]^{\frac{1}{n}} \left(\frac{\partial h}{\partial t}\right) \Big/ \left\{ \int_0^h \frac{(z'-e)^{\frac{1}{n}-1}}{[A(z')]^{\frac{1}{n}}}\, dz' \right\}, \quad 0 \le x < \delta(t), \quad t_I \le t \tag{31}$$

where A(h) is the reciprocal viscosity function A(z) evaluated at z=h.

We have thus obtained governing equations (26) subjected to interface equations (29), (30) and (31), and we must solve these equations for the unknowns M,h,δ, and e with boundary conditions (22). Although boundary conditions (22) are not applied at a moving boundary, we do have the interface equations which are applied at the moving junction. We shall thus use familiar terminology and call this problem a Stefan-like problem. It is readily seen that the present nonlinear problem is very complicated and numerically challenging; we shall present its numerical solution in the next section.

4. NUMERICAL TECHNIQUE AND RESULTS

4.1 Solution Technique

For convenience we introduce the following nondimensional variables:

$$\bar{t} = \frac{t}{t_I}\ , \ (\bar{t}_I=1) \qquad \bar{e} = \frac{e}{h_o} \qquad \bar{\delta} = \frac{\delta}{L}$$

$$\bar{x} = \frac{x}{L}\ , \ (0\leq\bar{x}\leq 1) \qquad \bar{D} = \frac{D}{D_{cr}}\ , \ (0\leq\bar{D}\leq 1)$$

$$\bar{z} = \frac{z}{h_o}\ , \ (0\leq\bar{z}\leq 1) \qquad \bar{A} = \frac{A(z)}{A(z=0)} \tag{32}$$

$$\bar{h} = \frac{h}{h_o}\ , \ (\bar{h}_o=1) \qquad \bar{\mathscr{\phi}} = \frac{\mathscr{\phi}}{\mathscr{J}^*}$$

$$\bar{w} = \frac{wK}{P_o} \qquad \bar{M} = \frac{M}{P_o L^2}$$

In the above, $\mathscr{J}^*$ represents the flexural rigidity of a beam at a uniform temperature T_u, where T_u is the temperature at the upper surface of the present non-uniform beam. Thus

$$\mathscr{J}^* = \frac{nbh^{\frac{1}{n}+2}}{2(2n+1)[2A(z=0)]^{\frac{1}{n}}} \tag{33a}$$

and

$$\bar{\mathscr{\phi}} = \frac{(1+2n)2^{\frac{1}{n}+1}}{n} \int_o^h \left[\frac{\bar{z}'-\bar{e}}{\bar{A}(\bar{z}')}\right]^{\frac{1}{n}} \bar{z}'\,d\bar{z}' \tag{33b}$$

We now follow the practice that unless otherwise noted all variables without bars appearing in this section from this point on will be dimensionless variables. In accordance with the above definitions, governing equation (18)

may be reformulated in terms of dimensionless variables as

$$\frac{\partial^5 M}{\partial x^4 \partial t} + B\left(\frac{M}{\mathscr{P}_o}\right)^n = 0 \tag{34}$$

in which we have introduced the dimensionless quantity

$$B = \frac{K t_I P_o^{n-1} L^{2n+2}}{\mathscr{P}_o^{*n}} \tag{35}$$

The variables appearing on the R.H.S. of eqn. (35) are all in dimensional form, and $\mathscr{P}_o^*$ is evaluated by setting $h=h_o$ in eqn. (33a). Note that the quantity B will be the key parameter in the present nondimensional study.

Employing the same techniques presented in [35], we may eliminate the spatial partial derivative appearing in eqn. (34) for the first stage. We thus obtain the integro-differential equations

$$\frac{\partial M}{\partial t} = \frac{B}{6}\left\{\int_o^x F(x,x')\left(\frac{M}{\mathscr{P}_o}\right)^n dx' + \int_o^1 G(x,x')\left(\frac{M}{\mathscr{P}_o}\right)^n dx'\right\} \tag{36a}$$

where

$$F(x,x') = -(x-x')^3 \tag{36b}$$

$$G(x,x') = 3x^2 - 3x^2x' - x'^3 + 3x'^2 - 2 \tag{36c}$$

The numerical solution to the above equation with geophysical data for a beam of constant thickness was presented in [35]. Here, we will employ a numerical

technique other than the one presented in [35]. A discretization scheme using the method of lines in space is obtained from the above eqn. (36a). It follows that

$$\frac{\partial M_i}{\partial t} = \frac{B}{\delta}\left\{\int_0^{x_i} F(x_i,x')\left(\frac{M}{\mathcal{J}_0}\right)^n dx' + \int_0^1 G(x_i,x')\left(\frac{M}{\mathcal{J}_0}\right)^n dx'\right\}, \qquad i=1,2,\ldots,N_2 \tag{37a}$$

$$\frac{\partial M_i}{\partial t} = 0 \qquad i=N_2+1 \tag{37b}$$

where

$$x_i = (i-1)\Delta x = \frac{1}{N_2}(i-1)$$

Note that the first integral in eqn. (37a) vanishes at i=1, eqn. (37b) corresponds to boundary condition (22b), and N_2 designates the number of spatial increments. Evaluating the integrals by the Newton-Cotes formulas, we thus obtain a system of ODE's which may be solved by Gear's stiff ODE algorithm [38]. The result obtained above furnishes the solution in the first stage of damage, and provides the initial data for the second stage of damage.

Returning now to eqns. (26), we may again integrate out the spatial derivatives to obtain for the thinning zone in the second stage

$$\frac{\partial M}{\partial t} = \frac{B}{\delta}\left\{\int_0^{x} F(x,x')\left(\frac{M}{\mathcal{J}}\right)^n dx' + \int_0^{\delta(t)} G(x,x')\left(\frac{M}{\mathcal{J}}\right)^n dx' + \int_{\delta(t)}^1 G(x,x')\left(\frac{M}{\mathcal{J}_0}\right)^n dx'\right\}, \qquad 0\le x<\delta(t), \quad 1\le t \tag{38a}$$

and for the uniform zone

$$\frac{\partial M}{\partial t} = \frac{B}{\delta}\left\{\int_{o}^{\delta(t)} F(x,x')\left(\frac{M}{\mathscr{J}}\right)^{n}dx' + \int_{\delta(t)}^{x} F(x,x')\left(\frac{M}{\mathscr{J}_o}\right)^{n}dx'\right.$$

$$\left. + \int_{o}^{\delta(t)} G(x,x')\left(\frac{M}{\mathscr{J}}\right)^{n}dx' + \int_{\delta(t)}^{1} G(x,x')\left(\frac{M}{\mathscr{J}_o}\right)^{n}dx'\right\}, \quad 0\leq x<\delta(t),\ 1\leq t \tag{38b}$$

where $\mathscr{J}$ was defined in (33b), and F(x,x'), G(x,x') were defined in eqns. (36 b,c). Note that we have used continuity of M and its derivatives at the junction point, e.g. $M(x=\delta(t)^{+},t) = M(x=\delta(t)^{-},t)$. In other words, the bending moment, shear force, deflection, and slope of the beam are all continuous at the junction point.

In order to mathematically fix the moving junction and the limits of integration appearing in eqns. (38), we employ the concept of Landau's transformation [39] and introduce the variable changes

$$\zeta = \frac{x}{\delta(t)}, \quad \text{for thinning zone} \qquad 0\leq x<\delta(t) \tag{39a}$$

$$\eta = \frac{x-\delta(t)}{1-\delta(t)}, \quad \text{for uniform zone} \qquad \delta(t)\leq x\leq 1 \tag{39b}$$

Under such a transformation the partial time derivative ∂( )/∂t is replaced by the substantial time derivative D( )/Dt in accordance with

$$\frac{\partial(\ )}{\partial t} = \frac{D(\ )}{Dt} - \frac{dx}{dt}\frac{\partial(\ )}{\partial x}$$

With the use of the chain rule, the transformed governing equations are obtained for the thinning zone as

$$\frac{DM}{Dt} = \frac{\zeta}{\delta(t)} \frac{d\delta(t)}{dt} \frac{\partial M}{\partial \zeta} + \frac{B}{6} \left\{ \delta(t) \int_0^{\zeta} F(\zeta,\zeta') \left(\frac{M}{\mathscr{J}}\right)^n d\zeta' + \delta(t) \int_0^1 G(\zeta,\zeta') \left(\frac{M}{\mathscr{J}}\right)^n d\zeta' \right.$$

$$\left. + [1-\delta(t)] \int_0^1 G(\zeta,\eta') \left(\frac{M}{\mathscr{J}_o}\right)^n d\eta' \right\}, \quad 0 \le \zeta < 1, \quad 1 \le t \tag{40a}$$

and for the uniform zone as

$$\frac{DM}{Dt} = \frac{1-\eta}{1-\delta(t)} \frac{d\delta(t)}{dt} \frac{\partial M}{\partial \eta} + \frac{B}{6} \left\{ \delta(t) \int_0^1 F(\eta,\zeta') \left(\frac{M}{\mathscr{J}}\right)^n d\zeta' + [1-\delta(t)] \int_0^{\eta} F(\eta,\eta') \left(\frac{M}{\mathscr{J}_o}\right)^n d\eta' \right.$$

$$\left. + \delta(t) \int_0^1 G(\eta,\zeta') \left(\frac{M}{\mathscr{J}}\right)^n d\zeta' + [1-\delta(t)] \int_0^1 G(\eta,\eta') \left(\frac{M}{\mathscr{J}_o}\right)^n d\eta' \right\}, \quad \begin{matrix} 0 \le \eta \le 1, \\ 1 \le t \end{matrix} \tag{40b}$$

Similarly, an application of Landau's transformation to interface equations (29),(31) yields

$$\frac{Dh}{Dt} = \frac{\zeta}{\delta(t)} \frac{d\delta(t)}{dt} \frac{\partial h}{\partial \zeta} - \left(\frac{M}{\mathscr{J}}\right)^n (h-e) \Big/ \left\{ \int_0^t \left[\frac{M}{\mathscr{J}}\right]^n dt' \right\}, \quad 0 \le \zeta < 1, \quad 1 \le t \tag{41}$$

and

$$\frac{De}{Dt} = \frac{\zeta}{\delta(t)} \frac{d\delta(t)}{dt} \frac{\partial e}{\partial \zeta} + n\left[\frac{Dh}{Dt} - \frac{\zeta}{\delta(t)} \frac{d\delta(t)}{dt} \frac{\partial h}{\partial \zeta}\right] \left[\frac{h-e}{A(h)}\right]^{\frac{1}{n}} \Big/$$

$$\left\{ \int_0^h \frac{(z'-e)^{\frac{1}{n}-1}}{[A(z')]^{\frac{1}{n}}} dz' \right\}, \quad 0 \le \zeta < 1, \quad 1 \le t \tag{42}$$

The transformed interface equation (30) has the slightly different form

$$\frac{d\delta(t)}{dt} = -\delta(t)M^n \Big/ \left\{ n \int_0^t M^{n-1} \frac{\partial M}{\partial \zeta}\, dt' \right\}, \quad \zeta=1, \quad 1 \leq t \tag{43}$$

since $\delta(t)$ involves only the single variable t. By virtue of variable changes (39), the substantial (material) time derivative $D(\ )/Dt$ appearing in the above transformed equations possesses a numerical value identical with $[\partial(\ )/\partial t]_\zeta$ or $[\partial(\ )/\partial t]_\eta$. It should be noted that fixing the moving junction unfortunately leads to governing equations of even more complicated form, and the above set of equations surely will not have a closed form solution. A numerical scheme will now be presented.

First, the method of lines in space [40] is utilized to eliminate the spatial derivatives from the above integro-differential equations in accordance with the discretization scheme shown in Fig. 2. Accordingly, we employ the central finite difference approximations for the interior points and one-sided three point formulas for the end points A,B and the junction point Q (see Fig. 2). Accordingly, eqns. (40-43) yield the following:

$$\frac{d\delta(t)}{dt} = -2\Delta\zeta\, \delta(t)\, M_i^n \Big/ \left\{ n \int_0^t M_i^{n-1}[M_{i-2}-4M_{i-1}+M_i]dt' \right\}, \qquad i=N_1+1 \tag{44}$$

$$\frac{DM_i}{Dt} = \frac{B}{\delta}\left\{ \delta(t) \int_0^1 G(\zeta_i,\zeta')\left(\frac{M}{\mathscr{M}}\right)^n d\zeta' + [1-\delta(t)] \int_0^1 G(\zeta_i,\eta')\left(\frac{M}{\mathscr{M}_0}\right)^n d\eta' \right\}, \quad i=1 \tag{45a}$$

$$\frac{DM_i}{Dt} = \frac{\zeta_i}{2\Delta\zeta\,\delta(t)}\frac{d\delta(t)}{dt}[M_{i+1}+M_{i-1}] + \frac{B}{\delta}\left\{ \delta(t) \int_0^{\zeta_i} F(\zeta_i,\zeta')\left(\frac{M}{\mathscr{M}}\right)^n d\zeta' \right. \tag{45b}$$

$$\left. + \delta(t) \int_0^1 G(\zeta_i,\zeta')\left(\frac{M}{\mathscr{M}}\right)^n d\zeta' + [1-\delta(t)] \int_0^1 G(\zeta_i,\eta')\left(\frac{M}{\mathscr{M}_0}\right)^n d\eta' \right\}, \quad i=2,3,\ldots,N_1$$

$$\frac{DM_i}{Dt} = \frac{\zeta_i}{2\Delta\zeta\,\delta(t)}\frac{d\delta(t)}{dt}\,[M_{i-2}-4M_{i-1}+3M_i] + \frac{B}{6}\left\{\delta(t)\int_0^{\zeta_i} F(\zeta_i,\zeta')\left(\frac{M}{\mathscr{P}}\right)^n d\zeta'\right.$$

$$\left. +\delta(t)\int_0^1 G(\zeta_i,\zeta')\left(\frac{M}{\mathscr{P}}\right)^n d\zeta' + [1-\delta(t)]\int_0^1 G(\zeta_i,\eta')\left(\frac{M}{\mathscr{P}_o}\right)^n d\eta'\right\}, \quad i=N_1+1 \qquad (45c)$$

$$\frac{DM_i}{Dt} = \frac{1-\eta_i}{2\Delta\eta[1-\delta(t)]}\frac{d\delta(t)}{dt}\,[M_{i+1}-M_{i-1}] + \frac{B}{6}\left\{\delta(t)\int_0^1 F(\eta_i,\zeta')\left(\frac{M}{\mathscr{P}}\right)^n d\zeta'\right.$$

$$+[1-\delta(t)]\int_0^{\eta_i} F(\eta_i,\eta')\left(\frac{M}{\mathscr{P}_o}\right)^n d\eta' + \delta(t)\int_0^1 G(\eta_i,\zeta')\left(\frac{M}{\mathscr{P}}\right)^n d\zeta'$$

$$\left. +[1-\delta(t)]\int_0^1 G(\eta_i,\eta')\left(\frac{M}{\mathscr{P}_o}\right)^n d\eta'\right\}, \quad i=N_1+2, N_1+3, \ldots, N_1+N_2 \qquad (45d)$$

$$\frac{DM_i}{Dt} = 0, \quad i=N_1+N_2+1 \qquad (45e)$$

$$\frac{Dh_i}{Dt} = -\left(\frac{M_i}{\mathscr{P}_i}\right)^n (h_i-e_i) \Big/ \left\{\int_0^t \left(\frac{M_i}{\mathscr{P}_i}\right)^n dt'\right\}, \quad i=1 \qquad (46a)$$

$$\frac{Dh_i}{Dt} = \frac{\zeta_i}{2\Delta\zeta\,\delta(t)}\frac{d\delta(t)}{dt}\,[h_{i+1}-h_{i-1}] - \left(\frac{M_i}{\mathscr{P}_i}\right)^n (h_i-e_i) \Big/ \left\{\int_0^t \left(\frac{M_i}{\mathscr{P}_i}\right)^n dt'\right\},$$

$$i=2,3,\ldots,N_1 \qquad (46b)$$

$$\frac{Dh_i}{Dt} = 0, \quad i=N_1+1 \qquad (46c)$$

$$\frac{De_i}{Dt} = n \frac{Dh_i}{Dt} \left[\frac{h_i - e_i}{A(h_i)}\right]^{\frac{1}{n}} \Big/ \left\{ \int_0^{h_i} \frac{(z'-e_i)^{\frac{1}{n}-1}}{[A(z')]^{\frac{1}{n}}} dz' \right\} , \qquad i=1 \tag{47a}$$

$$\frac{De_i}{Dt} = \frac{\zeta_i}{2\Delta\zeta\ \delta(t)} \frac{d\delta(t)}{dt} [e_{i+1} - e_{i-1}] + n\left[\frac{Dh_i}{Dt} - \frac{\zeta_i}{2\Delta\zeta\ \delta(t)} \frac{d\delta(t)}{dt} (h_{i+1} - h_{i-1})\right] \cdot$$

$$\left[\frac{h_i - e_i}{A(h_i)}\right]^{\frac{1}{n}} \Big/ \left\{ \int_0^{h_i} \frac{(z'-e_i)^{\frac{1}{n}-1}}{[A(z')]^{\frac{1}{n}}} dz' \right\} , \qquad i=2,3,\ldots,N_1 \tag{47b}$$

$$\frac{De_i}{Dt} = 0 , \qquad i=N_1+1 \tag{47c}$$

In the above

$$\zeta_i = (i-1)\Delta\zeta = \frac{1}{N_1} (i-1) , \qquad i=1,2,\ldots,N_1$$

$$\eta_i = (i-N_1-1)\Delta\eta = \frac{1}{N_2} (i-N_1-1) , \qquad i=N_1+1, N_1+2, \ldots, N_1+N_2+1$$

$$\Delta\zeta = \frac{1}{N_1} , \qquad \Delta\eta = \frac{1}{N_2}$$

and N_1, N_2 designates, respectively, the number of spatial increment in thinning zone and uniform zone, and $\mathcal{J}_i$ is obtained by setting $h=h_i$ is eqn. (33b).

Note that eqn. (45e) corresponds to boundary condition (22b). Moreover, Dh/Dt and De/Dt as given by eqns. (46c) and (47c) vanish at the junction point, since at any instant we always have h=1 and $e=e_o$ at this point. The

integrals appearing in the above set of equations were evaluated by use of the Newton-Cotes formulas. We thereby obtained a large system of $3N_1+N_2+4$ ordinary differential equations. A computer program was developed first to solve eqn. (23) for e_o and then to solve eqns. (37) for the M_i's using the initial bending moment function (see Sec. 4.2) as the initial condition. We then used these results along with $h_i=1$, $e_i=e_o$, $\delta=0$ as the initial conditions to solve the system of ODE's, eqns. (44-47).

It is also useful to compute the deflection of the beam. This can be accomplished by substituting the above bending moments M_i into the nondimensinal form of the equation of equilibrium

$$\frac{\partial^2 M}{\partial x^2} = -P + Kw$$

However, this approach leads to considerable numerical error due to the presence of the derivative term in the above equation. An alternate and more accurate approach is to develop differential equations in the deflection. The same solution technique used for the bending moment is also applicable to these differential equations in the deflection. For the sake of brevity, the resulting equations will not be presented here (see [18]). An even larger system of $4N_1+2N_2+5$ ODE's is obtained in this case. A high accuracy yet costly numerical algorithm, i.e. Gear's stiff ODE algorithm, was used to solve this system.

4.2 Solutions and Discussion

Our attention is first directed to a special case in which closed form solutions exist. Thus, let us delete the elastic Winkler foundation and also consider a beam with a uniform temperature distribution equal to T_u (a dimensional quantity). Under such circumstances, the bending moment M remains constant in time, and the neutral axis coincides with the centroidal axis owing to the homogeneous nature of the material properties. Moreover, we have the following values for the dimensionless quantities [see eqns. (32) and (33)]

$$e = \frac{1}{2} h$$

$$A(z) = 1$$

$$\mathcal{J} = h^{\frac{1}{n}+2}$$

The dimensionless governing equations for h,e [see eqns. (29) and (31)] in the thinning zone ($0 \leq x < \delta(t)$) follow for this special case as

$$\frac{\partial h}{\partial t} = - \frac{h^{-2n}}{2 \int_0^t h^{-1-2n} dt'} , \qquad 1 \leq t \tag{48a}$$

$$\frac{\partial e}{\partial t} = 2 \frac{\partial h}{\partial t} , \qquad 1 \leq t \tag{48b}$$

and that for $\delta(t)$ becomes

$$\frac{d\delta(t)}{dt} = - \frac{M}{nt \frac{\partial M}{\partial x}} \qquad x = \delta(t) , \quad 1 \leq t \tag{48c}$$

Note that these equations may be solved consecutively and that eqns. (48 a,b) include neither the x variable nor the input load function P(x,t) explicitly. Physically, eqn. (48b) indicates that although $2e_o=h_o=1$ initially, both quantities will be equal to zero at the instant the beam collapses. After eliminating the integral via differentiation, eqn. (48a) may be rewritten as

$$\frac{\partial}{\partial t}\left[\frac{\partial h}{\partial t}\cdot h^{2n-2}\right]=0 \tag{49}$$

This differential equation may be solved analytically with the initial conditions

$$h = 1 \qquad \text{at} \qquad t = t_I$$

and

$$\frac{\partial h}{\partial t} = -\frac{1}{2t_I} \qquad \text{at} \qquad t = t_I$$

where $t_I=t_I(x)$ designates the time required for a material point with coordinates (x,1) to reach the critical state. The second initial condition in the above was obtained by setting $t=t_I$ and h=1 in eqn. (48a). The solution to eqn. (49) is then obtained as

$$\frac{t}{t_I(x)} = \frac{2}{1-2n}h^{2n-1} - \frac{1+2n}{1-2n}, \qquad 0\leq x<\delta(t), \qquad 1\leq t \tag{50}$$

which is identical to the result derived in [8].

The solution to eqn. (48b) for e then follows directly from the solution of eqn. (50) for h. Here $t_I(x)$ may be expressed in terms of the bending moment M(x). Since the point (0,1) reaches the critical state at time t=1 while the point (x,1) ruptures at time $t=t_I(x)$, it follows from eqn. (25) that

$$t_I(x) = (\frac{M_o}{M})^n \tag{51}$$

Here, M_o and M represent the bending moments at points with x-coordinates equal to 0 and x, respectively. Equation (50) thus becomes

$$(\frac{M}{M_o})^n t = \frac{2}{1-2n} h^{2n-1} - \frac{1+2n}{1-2n} , \quad 0 \leq x < \delta(t) , \quad 1 \leq t \tag{52}$$

Although differential equation (48a) in h does not explicitly involve the variable x and the bending moment M, its solution (52) is seen to be directly related to M.

The function $t_I(x)$ in eqn. (51) may be inverted in the simple case that the bending moment M(x) is monotonic in nature. In fact, for such a simple case the constraint on the moving juntion

$$x = \delta(t)$$

is invertible and is physically equivalent after inverstion to

$$t = t_I(x)$$

Consequently, witht he use of eqn. (51), eqn. (48c) attains the alternate form

$$\frac{d\delta(t)}{dt} = - \frac{M^{n+1}}{nM_o^n \frac{\partial M}{\partial x}} , \quad x=\delta(t) , \quad 1 \leq t \tag{53}$$

Consider for the moment a very simple case in which a point-load is applied on the beam at x=0. The bending moment for this load is simply given as

$$M = M_o(1-x) \tag{54}$$

and differential equation (53) becomes

$$\frac{d\delta(t)}{dt} = \frac{1}{n}\,[1-\delta(t)]^{n+1}\,, \qquad 1 \leq t$$

With the initial condition δ at t=1 equal to 0, the above equation yields the solution

$$\delta(t) = 1 - t^{-\frac{1}{n}}\,, \qquad 1 \leq t \tag{55}$$

Note that solution (55) is also obtainable from the solution (52) by setting h=1 and using expression (54). The solutions of this special closed-form case are now complete.

We thus turn our attention to the original problem, containing in general both the Winkler term and a temperature gradient. A singularity appears in eqn. (39a) at time t=1 when δ=0, and this leads to numerical difficulties. This obstacle may be circumvented by introducing an "imperfection" [33] in eqn. (39a). Here, we follow the latter approach and introduce an imperfection in δ as

$$\delta(t) = 1.0\text{x}10^{-6} \qquad \text{at} \quad t=1$$

Moreover, the temperature in the beam is assumed to be linearly distributed in the z-direction in accordance with (see Fig. 1c)

$$T = T_u + (T_b - T_u)z\,, \qquad 0 \leq z \leq 1$$

where the dimensional surface and bottom temperatures are chosen respectively as

$$T_u = 300^{o}k \ , \quad T_b = 360^{o}k$$

Also, we use for the creep activation energy the dimensional value

$$\Delta H = 0.112x10^{6} \ J \cdot mole^{-1}$$

Note that because of the nondimensional form of our governing equations it was not necessary to stipulate a specific material. Finally the number of increments chosen in the present beam problem were

$N_1 = 5$ for the thinning zone

$N_2 = 10$ for the uniform zone

which yield a total of 29 ODE's, or 45 if the equations for deflection are also included. In order to limit the complexity of this nonlinear problem, only the uniformly applied load is considered here. In this case, the shape function [see eqn. (20)] of the applied load is simply

$$f(x) = 1 \ , \qquad 0 \leq x \leq 1$$

The initial bending moment function $M(x,0^{+})$ is obtainable from eqns. (21) and (22), and is given as

$$M(x,0^{+}) = (x^{2}-1)/2 \tag{56}$$

which will be used as the initial condition for eqns. (37).

The results we shall present may be separated into two groups, i.e. those with the foundation present and those with the foundation absent. In the

latter case of the foundation absent, we have from eqn. (35) B=0 since in this case the spring constant for the foundation is identically zero. We consider the B=0 case first, and note that here the bending moment is independent of time, and is thus given simply by eqn. (56) after the lateral load is applied. (For the B=0 case, we did not calculate the deflection of the beam.) Figures 3 and 4 display the propagating rupture front for B=0 in the second stage of damage for n=3 and 5, respectively. In these figures the depth and axial coordinates z,x of the beam are given in nondimensional form. The sequence of curves inside the beam trace the propagation of the rupture front as time ellapses. The $\delta(t)$ function at time t is given by the distance along the bottom surface (z=1) from the point x=0 to the intersection of the curve for time t with the bottom surface. Note that the beam of n=3 material exhibits a wider thinning zone than does the beam of n=5 material. It would appear that the rupture front of the n=5 beam propagates faster than that of the n=3 beam. But you are reminded that this observation is made for a nondimensional time scale and will not necessarily follow for dimensional time. Each set of these curves for a parameter n required about 1 minute of computer time (CPU).

We now turn to the general case with the Winkler foundation present. The dimensionless parameter B [see eqn. (35)] contains a group of constants including the spring constant of the foundation, applied load, geometry and material properties of the beam, and is considered arbitrary in the present nondimensional study. Here we chose for illustration the value B=1 which requires that the numerator and denominator in eqn. (35) be of the same order. In addition to the bending moment M, we also computer the deflection w

for this case. Due to the complicated nature of the governing large system of ODE's, a considerable amount of computer time was required to complete one run for a specific value of n. Thus we limited the computer time to 1000 seconds (about 16.7 minutes) per run, and accordingly obtained a reasonable number of solution curves for time steps in the early part of the second stage of damage. The computations could have easily been extended up to the point of final collapse of the beam, but for reasons of economy this was not done.

Figures 5a,b give respectively the nondimensional deflection of the beam for values 3 and 5 for the stress power n. Since the chosen load is uniformly distributed, these curves do not exhibit the characteristic "uplift" which often occurs under centrally concentrated loads or point loads on a beam with a Winkler foundation [34, 35]. According to the flexural model presented in [35], the deflections of a beam which experiences no damage approaches an asymptotic limit as the time tends to infinity. However, no asymptotic deflection solution exists in the present problem, since damage causes the beam to thin and accordingly the deflection is unbounded. This may readily be seen in Fig. 5b, in which the increment of beam deflection is clearly increasing in the final few time steps shown. Although we have used Norton's steady creep law, eqn. (16), to describe the creep behavior of the material, the nature of the deflection shown in Fig. 5b is similar in form to the typical creep curve with its three stages of creep. Such behavior coincides with the recent experimental investigations [41, 42] in which a beam with a deep notch was subjected to a uniform temperature and point load. This can be explained by the fact that as the beam starts thinning the remaining material carries the same load but with greater stress.

In [35] where no damage was included, McMullen et al noted that the bending moment relaxes after the load is applied and approaches zero as time tends to infinity. Figures 6a,b exhibit this same relaxation of the bending moment in the more general case where damage causes the beam to thin. Furthermore, Fig. 6b shows that the relaxation of the bending moment accelerates in the final few time steps shown; it is believed that Fig. 6a would also do the same if the computer time had been extended. Since the lifetime of the beam is finite, the beam should collapse before the bending moment vanishes. Figures 7a,b display the propagating rupture front for B=1 with n=3 and 5, respectively. As in the B=0 case, the rupture fronts in the present case have sharper profiles in the n=5 beam than in the n=3 beam. And the rupture front for the n=5 beam propagates faster than that for the n=3 beam relative to the nondimensional time scale. We also point out that the numerical scheme for the system of ODE's presented in the previous section is stiffer for n=5 than that for n=3, since within the chosen limit of compute time (100 seconds) the final time step reached was t=1.90 for the case of n=3 and only t=1.60 for the case of n=5.

It should be noted that the results displayed may contain some numerical error in the later time intervals, since we are restricted by the limitations of infinitesimal strain and small rotations. Although we have formulated the problem in an idealized manner, a significant amount of mathematical difficulty was still encountered. If one attemps to relax some of the assumptions imposed, the complexity of the problem could increase greatly and possibly preclude a successful numerical analysis.

REFERENCES

1. F.R. Larson and J. Miller, A Time-Temperature Relation for Rupture and Creep Stresses, Trans. A.S.M.E., Vol. 174, pp. 765-775, 1952.
2. S.S. Manson and A.M. Haferd, A Linear Time-Temperature Relation for Extrapolation for Creep and Stress Rupture Data, N.A.C.A. TN 2890, 1953.
3. R.L. Orr, O.D. Sherby and J.E. Dorn, Correlations of Rupture Data for Metals at Elevated Temperatures, Trans. ASM, Vol. 46, pp. 113-128, 1954.
4. S.S. Manson and C.R. Ensign, A Quarter-Century of Progress in the Development of Correlation and Extrapolation Methods for Creep Rupture Data, J. Eng. Mat. Tech., Vol. 101, pp. 317-325, 1979.
5. J.B. Conway, Stress-Rupture Parameters: Origin, Calculations and Use, Gordon and Breach, New York, 1969.
6. E.L. Robinson, Effect of Temperature Variation on the Long-Time Rupture Strength of Steels, Trans. A.S.M.E., Vol. 74, pp. 777-781, 1952.
7. N.J. Hoff, The Necking and Rupture of Rods Subjected to Constant Tensile Loads, J. of Applied Mechanics, Vol. 20, pp. 105-108, 1953.
8. L.M. Kachanov, Rupture Time Under Creep Conditions, Problems of Continuum Mechanics, contributions in honor of seventieth birthday of N.I. Muskhelishville, (ed. J.R.M. Radok), SIAM, Philadelphia, p. 202-218, 1961.
9. Y.N. Robotnov, Creep Rupture, Proc. 12th Int. Congr. Appl. Mech., Springer-Verlag, Berlin, 1969.
10. F.A. Leckie and D.R. Hayhurst, Creep Rupture of Structures, Proc. Roy. Soc. Londen, A340, pp. 323-347, 1974.
11. F.A. Leckie and D.R. Hayhurst, Constitutive Equations for Creep Rupture, Acta Metall, Vol. 25, pp. 1059-1071, 1977.
12. F.K.G. Odqvist, Mathematical Theory of Creep and Creep Rupture, 2nd edn., Oxford Clarendon Press, Oxford, 1974.

13. R. Penny and D. Marriot, Design for Creep, McGraw-Hill, New York, 1971.

14. G. Piatti, R. Lubek and R. Matera, The Measurement of Small Density Variations in Solids, JRC Techn. Note N.I.77.6 173/2. 10.1/3, Mar 1977.

15. G. Belloni, G. Bernasconi and G. Piatti, Damage and Rupture in AISI 310 Austenitic Steel, Meccanica, Vol. 12, pp. 84-96, 1977.

16. G. Belloni, G. Bernasconi and G. Piatti, Creep Damage Models, In Creep in Engineering Materials and Structures (eds. G. Bernasconi and G. Piatti), Ch.8, pp. 195-229, Applied Science Publ., London, 1980.

17. D.A. Woodford, A Parametric Approach to Creep Damage, Met. Sci, J., Vol. 3, pp. 50-53, 1969.

18. R.J. Gu, Strain-Controlled Creep Rupture in Non-Isothermal Materials, Ph.D. Dissertation, State University of New York at Buffalo, Sept 1984.

19. M.N. Ozisik, Heat Conduction, Wiley, New York, 1980.

20. G. Schoeck, Theories of Creep, in Mechanical Behavior of Materials at Elevated Temperatures (ed. J.E. Dorn), McGraw-Hill, 1961.

21. M. Ashby, A First Report on Deformation-Mechanism Maps, Acta Metall., Vol. 20, pp. 887-897, 1972.

22. M. Ashby, Strengthening Methods in Metals and Alloys, in The Microstructure and Design of Alloys, Proc. 3rd Int. Conf. on Strength of Metals and Alloys, Cambridge, England, Vol. 2, pp. 8-42, 1973.

23. R. Raj and M.F. Ashby, On Grain Boundary Sliding and Diffusion Creep, Metall. Trans., Vol. 2, pp. 1113-1127, 1971.

24. G.H. Edward and M.F. Ashby, Intergranular Fracture During Power-Law Creep, Acta Metall., Vol. 27, pp. 1505-1518, 1979.

25. A.K. Mukherjee, J.E. Bird and J.E. Dorn, Experimental Correlations for High-Temperature Creep, Trans. ASM, Vol. 62, pp. 155-179, 1969.

26. C.S. Lee, F.A. Cozzarelli and K. Burke, One-Dimensional Strain-Dependent Creep Damage in Inhomogeneous Materials, to appear in Int. J. Nonlinear Mechanics.

27. G. Piatti, G. Bernasconi, and F.A. Cozzarelli, Damage Equations for Creep Rupture in Steels, Proc. 5th Int. Conf. in Reactor Technology, paper L11/4, Berlin, August, 1979.

28. F.C. Monkman and N.J. Grant, An Impirical Relationship Between Rupture Life and Minimum Creep Rate in Creep Rate in Creep-Rupture Tests, Proc. ASTM, 56, 593, 1956.

29. H.D. Hanna and G.W. Greenwood, Cavity Growth and Creep in Copper at Low Stresses, Acta Metall., Vol. 30, pp. 719-724, 1982.

30. F.A. Cozzarelli and G. Bernasconi, Nonlinear Creep Damage Under One-Dimensional Variable Tensile Stress, Int. J. Non-Linear Mechanics, Vol. 16, No. 1, pp. 27-38, 1981.

31. K. Burke and F.A. Cozzarelli, On The Thermodynamic Foundations of Strain-Dependent Creep Damage and Rupture in Three Dimensions, Int. J. Solids Structures, Vol. 20, No. 5, pp. 487-497, 1984.

32. A.E. Johnson, J. Henderson and B. Khan, Complex-Stress Creep, Relaxation and Fracture of Metallic Alloys, H.M.S.O., Edinburg, 1962.

33. R.M. Furzeland, A Comparative Study of Numerical Methods for Moving Boundary Problems, J. Inst. Math. Applics., Vol. 26, pp. 411-429, 1980.

34. W. Flugge, Viscoelasticity, 2nd revised edn., Springer-Verlag, New York, 1975.

35. R.J. McMullen, D.S. Hodge and F.A. Cozzarelli, A Technique for Incorporating Geothermal Gradients and Nonlinear Creep into Lithospheric Flexure Models, J. of Geoph. Research, Vol. 86, pp. 1745-1753, 1981.

36. I.Finnie and W.R. Heller, Creep of Engineering Materials, McGraw-Hill, 1959.

37. P. Schiller, D. Boerman, P. Fenici, R. Matera, G. Pellegrini, G. Piatti and E. Ruedl, Testing and Modeling of Mechanical Properties of Metals, Highlights of Materials Science, EUR-5508, pp. 53-67, 1973-76.

38. C.W. Gear, Numerical Integration of Stiff Ordinary Differential Equations, Report No. 221, Dept. of Computer Science, University of Illinois, 1967.

39. H.G. Landau, Heat Conductions in a Melting Solid, Quart. of Appl. Math., Vol. 8, pp. 81-94, 1950.

40. R.M. Furzeland, Analysis and Computer Packages for Stefan Problems, Internal Report, Oxford University Computing Laboratory, 1979.

41. V.M. Radhakrishnan and A.J. McEvily, A Critical Analysis of Crack Growth in Creep, Trans, ASME, J. of Engg. Mat. and Tech., Vol. 102, pp. 200-206, 1980.

42. V.M. Radhakrishnan and A.J. McEvily, Effect of Temperature on Creep Crack Growth, Trans. ASME, J. of Engg. Mat. and Tech., Vol. 102, pp. 350-355, 1980.

1288G

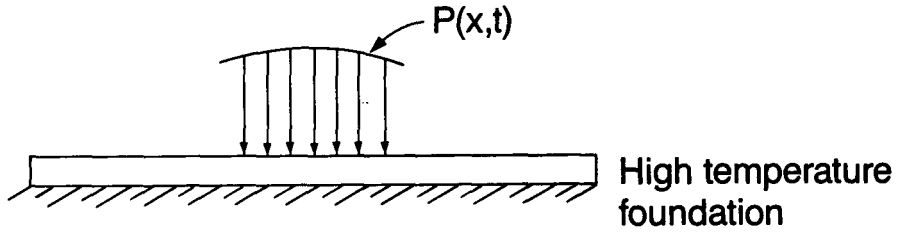

Fig. 1a Beam on high temperature foundation, subjected to lateral load P(x,t).

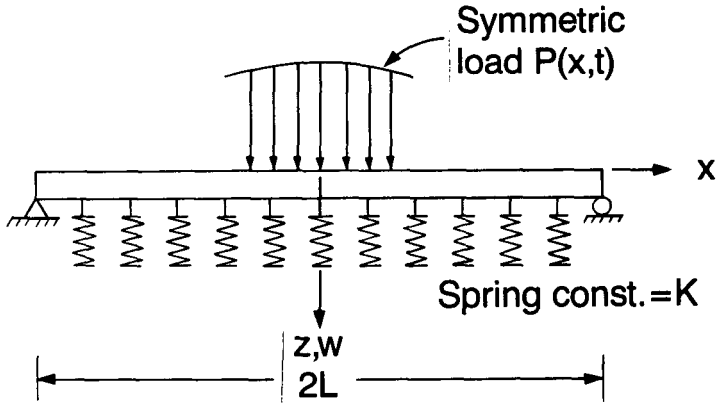

Fig. 1b Beam with simple end supports, elastic Winkler foundation, and symmetric load.

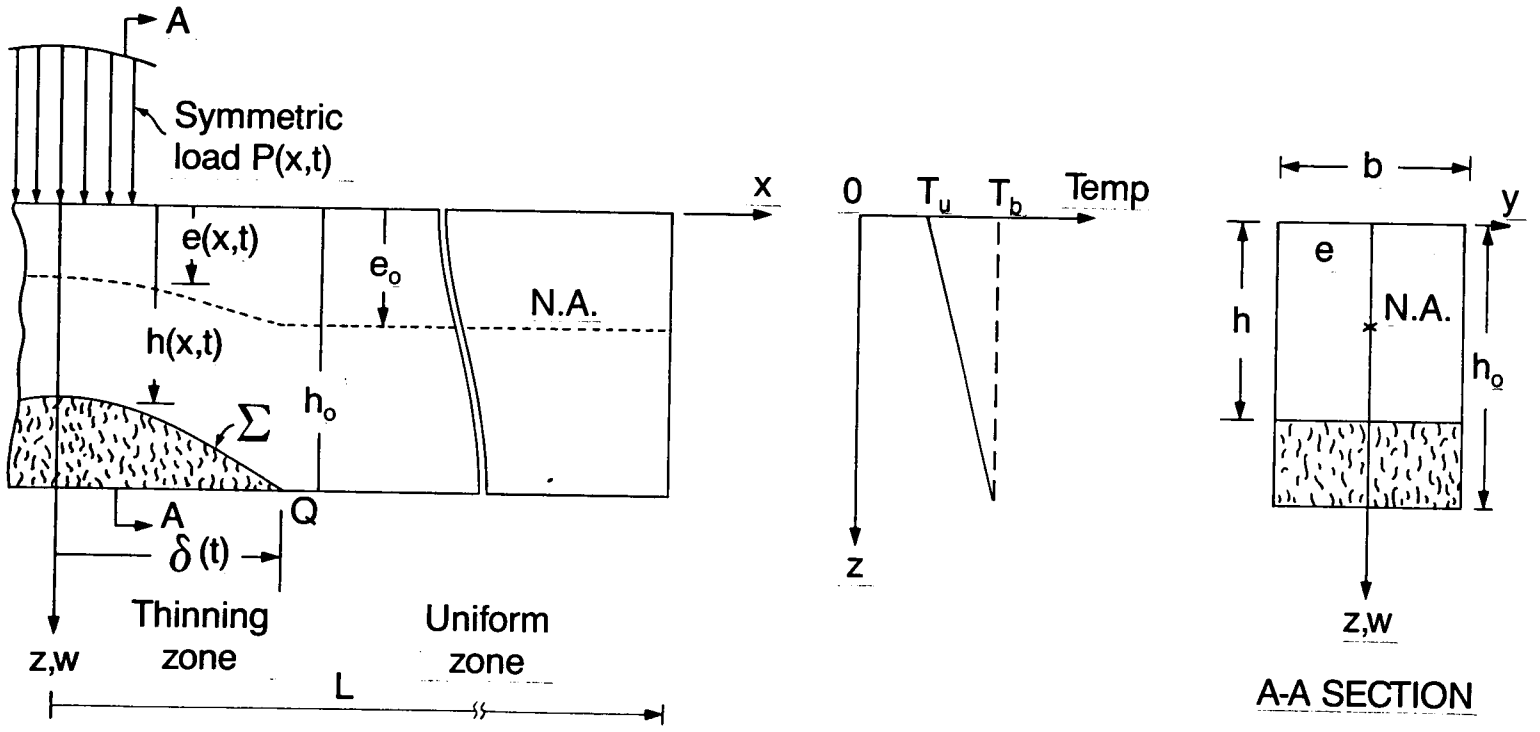

Fig. 1c Propagation of the rupture front and the linear temperature profile.

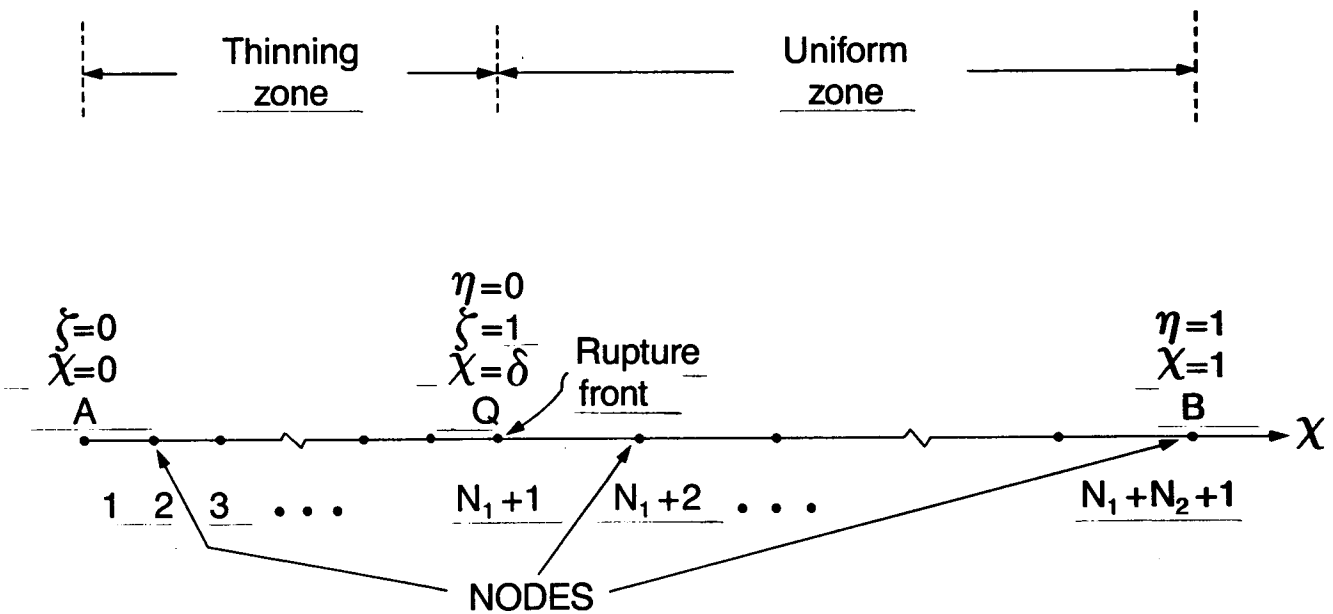

Fig. 2 Variable network in the second stage of creep damage.

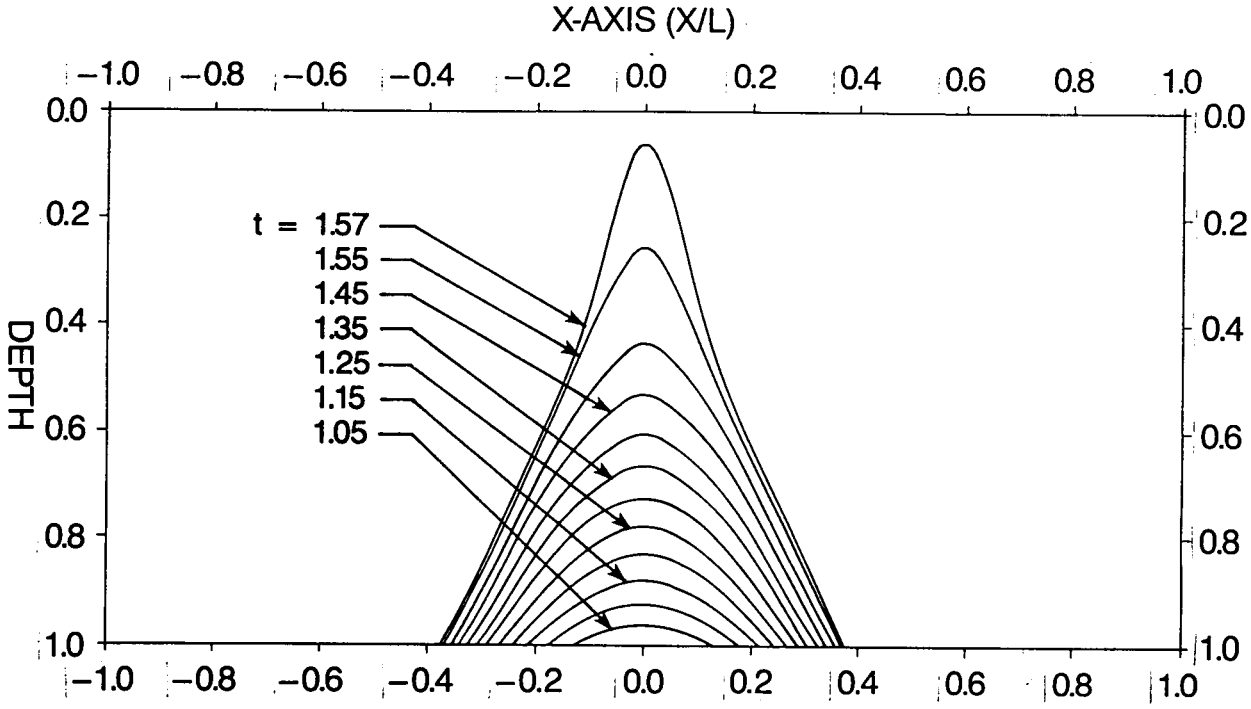

(a)

Fig. 3 Propagation of rupture front in a beam with no Winkler foundation — (a) B=0 and n=3, (b) B=0 and n=5.

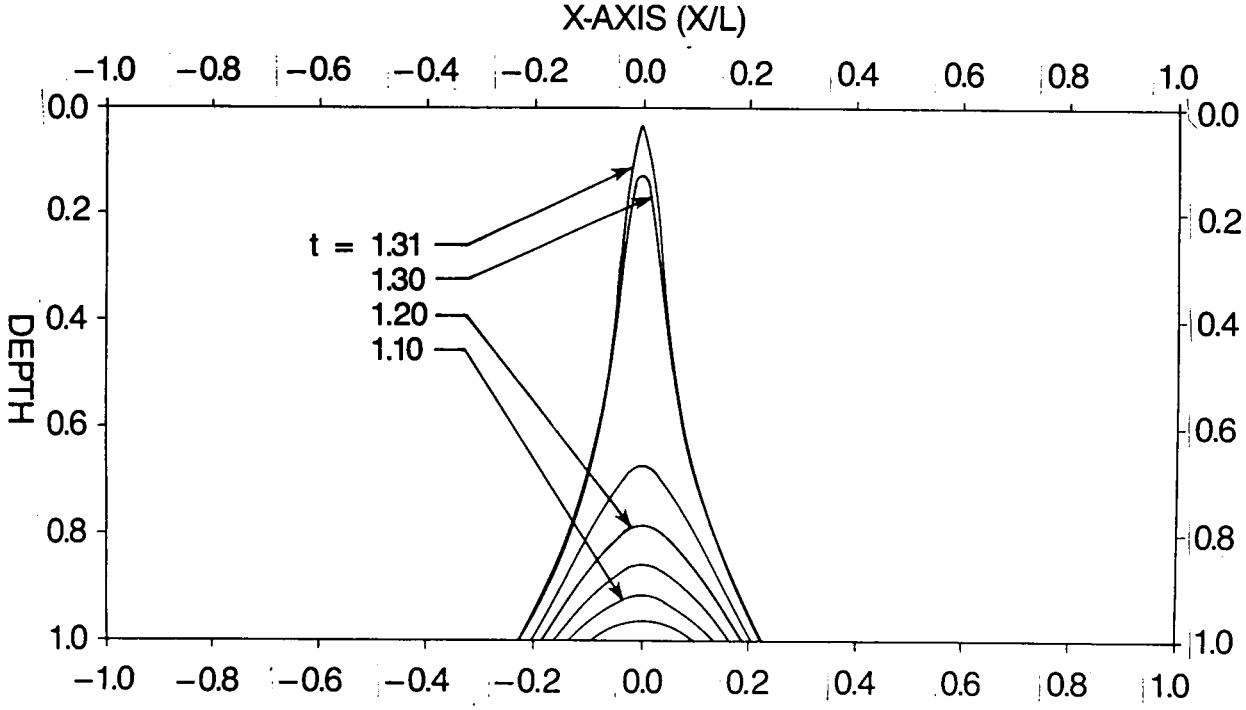

(b)

Fig 3. (continued)

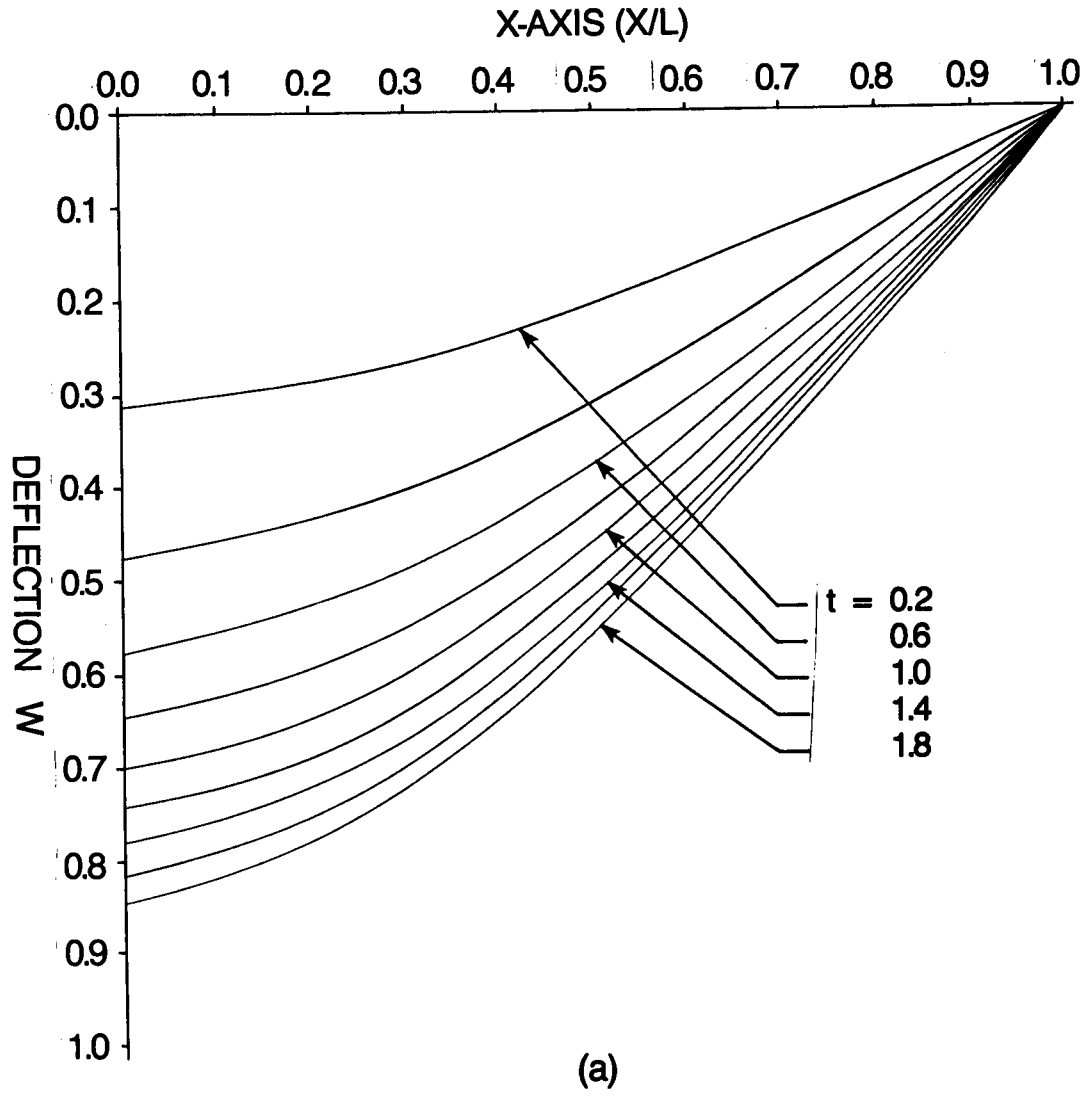

Fig. 4 Nondimensional deflection of a beam resting on Winkler foundation — (a) B=1, n=3, T_b=360°k and T_u=300°k, (b) B=1, n=5, T_b=360°k and T_u=300°k.

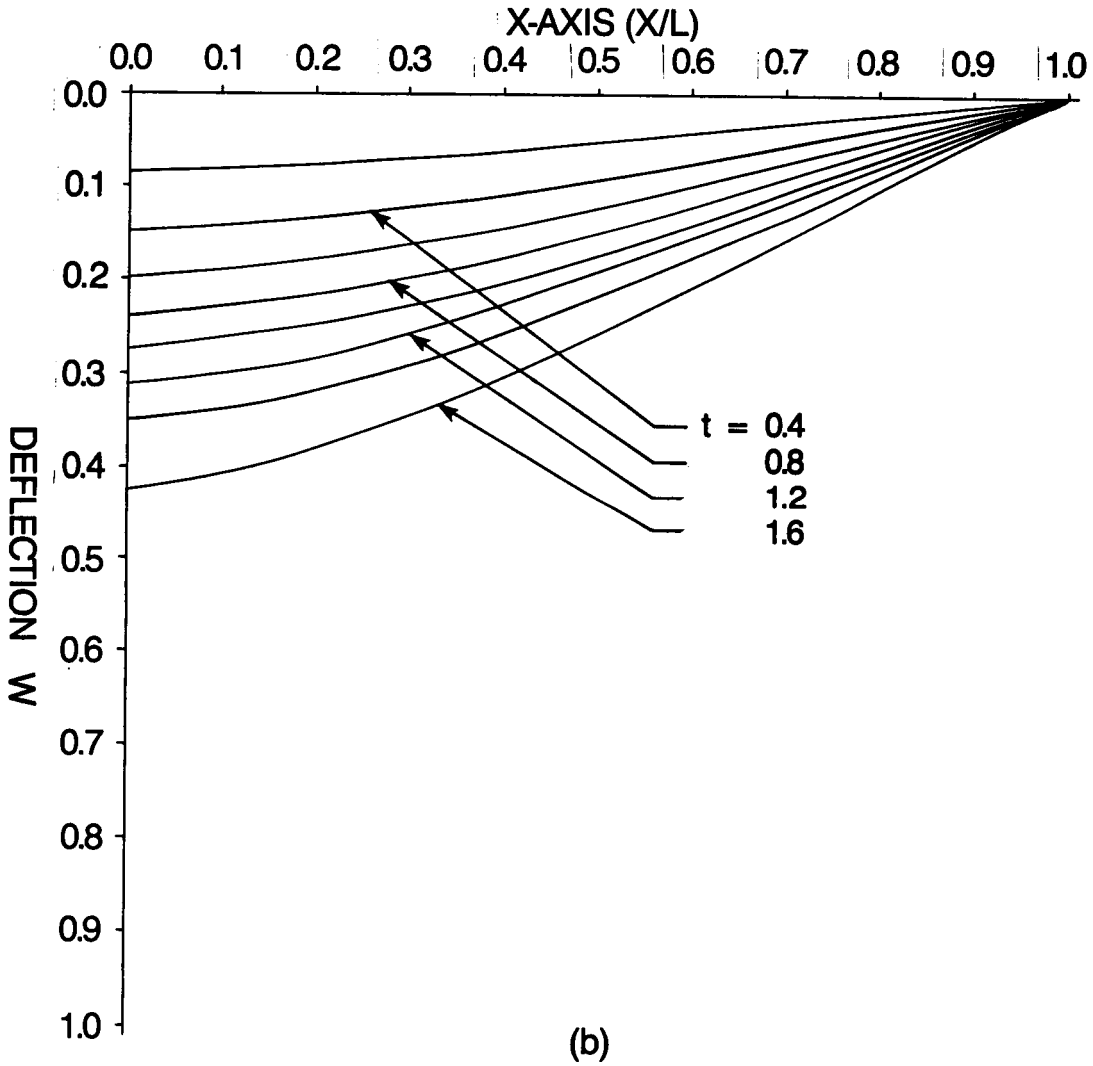

(b)

Fig 4. (continued)

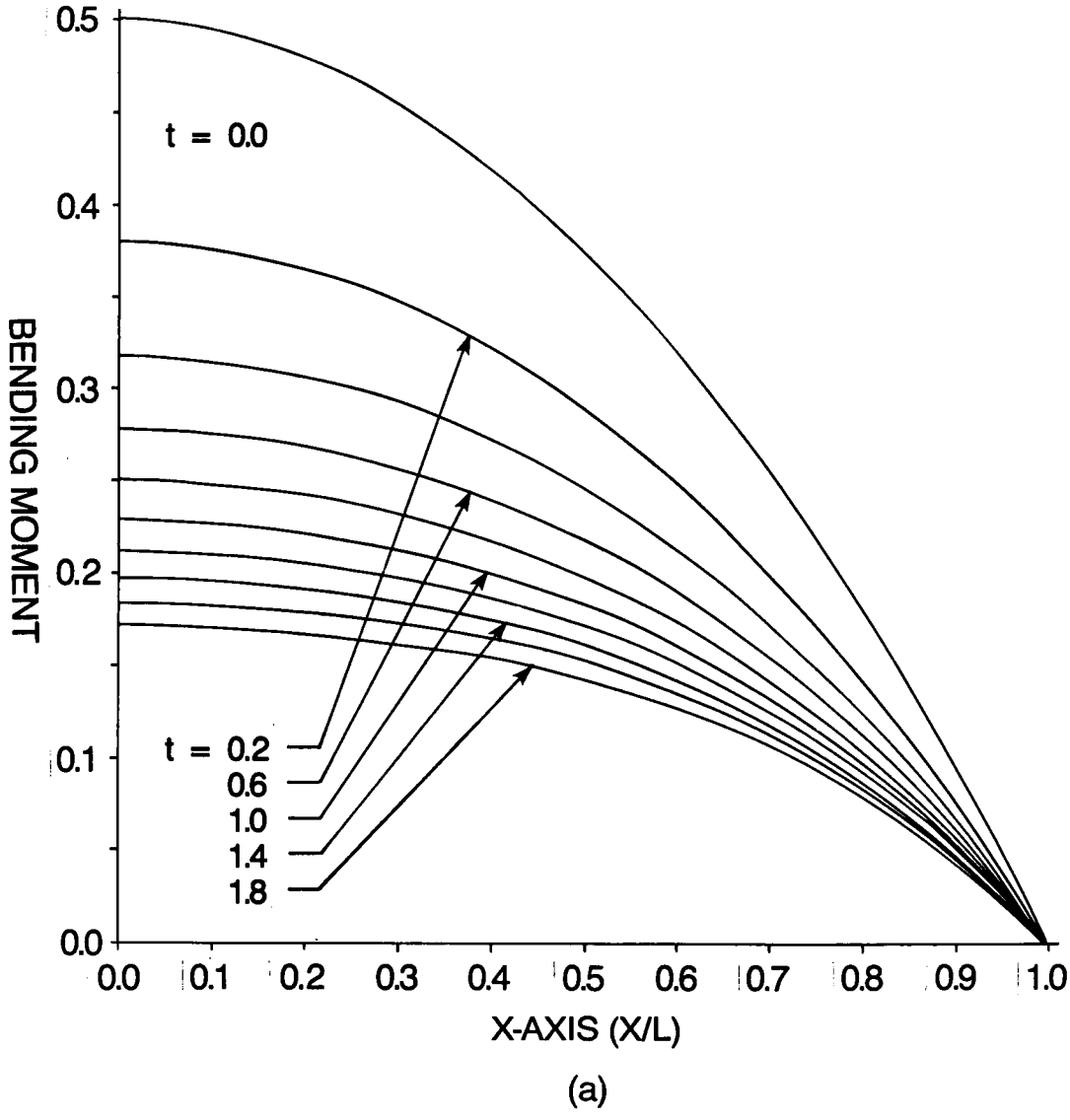

(a)

Fig. 5 Nondimensional bending moment along a beam on Winkler foundation — (a) B=1.0, n=3, T_b=360°k and T_u=300°k, (b) B=1.0, n=5, T_b=360°k and T_u=300°k.

Fig. 5 (continued)

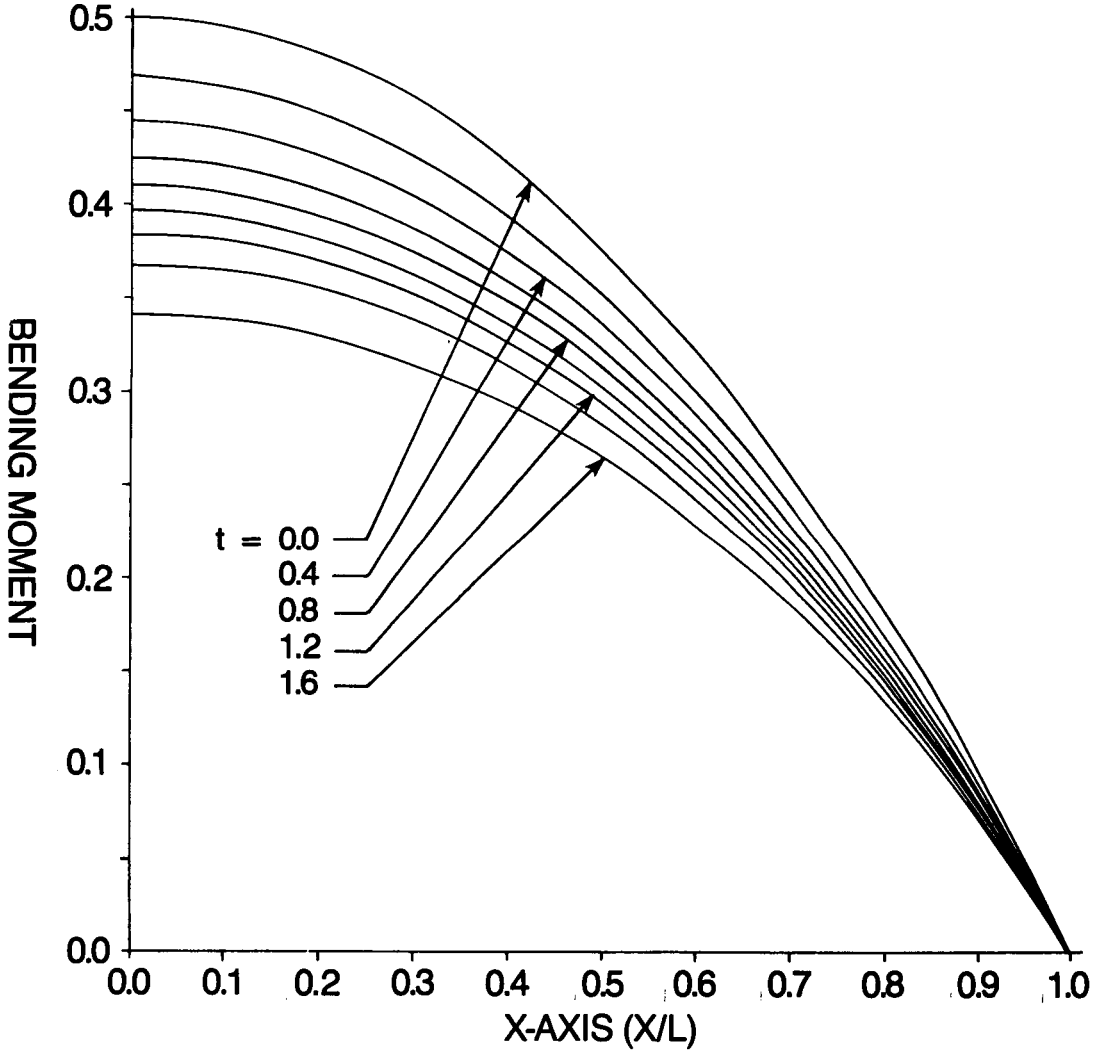

(b)

C-3

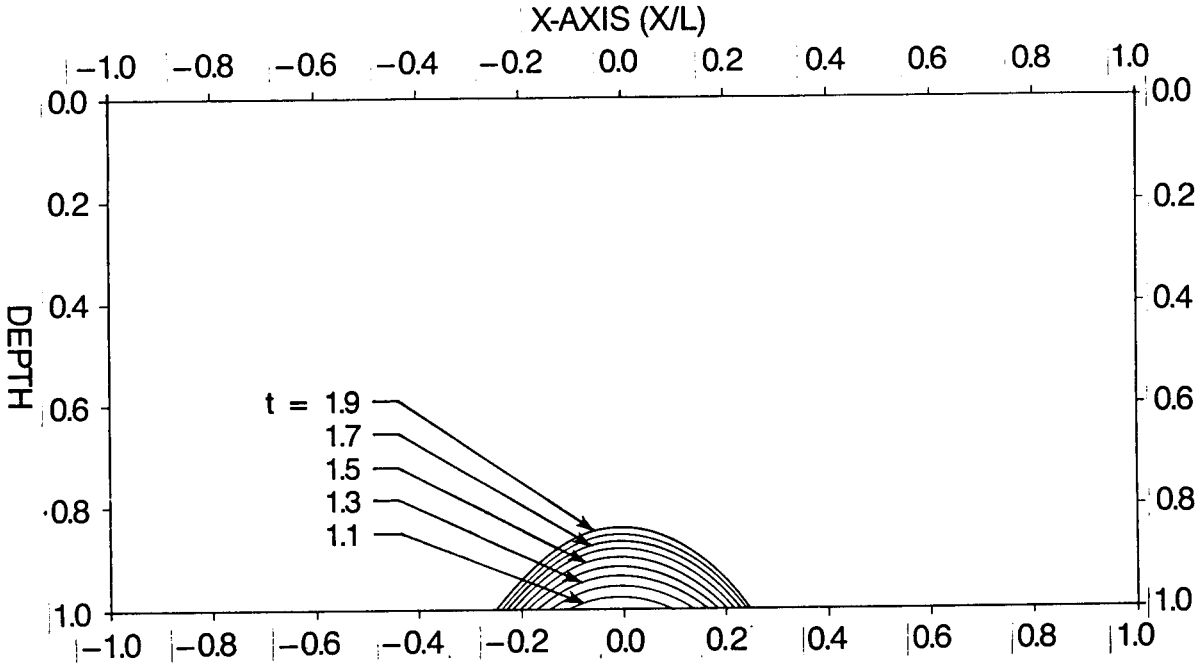

(a)

Fig. 6 Propagation of rupture front in a beam on Winkler foundation — (a) B=1, n=3, T_b=360°k and T_u=300°k, (b) B=1, n=5, T_b=360°k and T_u=300°k.

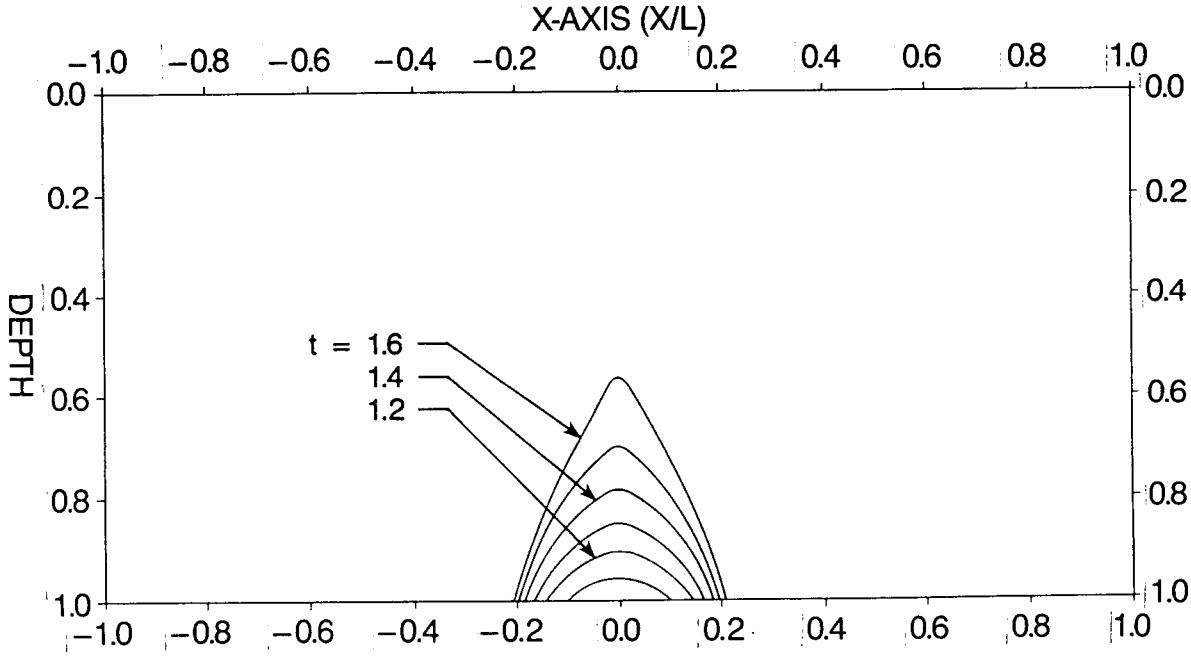

(b)

Fig. 6 (continued)